

CART Expression and Gastric Ulcerations

Subjects: Genetics & Heredity

Contributor: Michal Zalecki

Cocaine- and amphetamine-regulated transcript (CART) is a peptide suggested to play a role in gastrointestinal tract tissue reaction to pathology. Gastric ulceration is a common disorder affecting huge number of people, and additionally, it contributes to the loss of pig livestock production. Importantly, ulceration as a focal disruption affecting deeper layers of the stomach wall differs from other gastrointestinal pathologies and should be studied individually. The pig's gastrointestinal tract, due to its many similarities to the human counterpart, provides a valuable experimental model for studying digestive system pathologies. To date, the role of CART in gastric ulceration and the expression of the gene encoding CART in porcine gastrointestinal tube are completely unknown.

Keywords: cocaine- and amphetamine-regulated transcript ; CART ; enteric nervous system ; stomach ; ulcer ; Q-PCR ; immunohistochemistry

1. Introduction

Cocaine- and amphetamine-regulated transcript (CART), a relatively recently discovered peptide, is being recognized as a substance playing an important role in the peripheral nervous system and is known to be expressed in nerves supplying various organs, especially the digestive tract. Importantly, its role in tissue reaction to pathological circumstances has been also observed, indicating its potential role in adaptive changes of tissues to pathology. Neuronal tissue is known to possess a special ability to respond to a pathological factor, which is referred to as 'neuronal plasticity'. Stomach, as a part of the digestive tract, is widely innervated by extrinsic and intrinsic nerves, and the later form a complicated and highly autonomic enteric nervous system ^[1]. Multiple experiments have revealed the reaction of enteric neurons to pathology, which was manifested by changes in expression of different neuropeptides by intrinsic nerve cells ^[2]. It should be stressed, that gastrointestinal tissue and nerve reactions are highly specific and strongly dependent on the influencing factor and the part of the intestinal tube ^{[1][2]}. Importantly, CART-dependent reaction to pathology was studied in the intestinal tissues ^{[3][4][5][6][7][8][9][10]}, while only occasional studies dealt with gastric tissues. The only available studies verified the changes in CART-immunoreactive stomach neurons during experimentally induced diabetes mellitus type I ^[11], intoxication with T2 toxin ^[12], acrylamide ^[13], and bisphenol a ^[14] supplementation, which are all multi-system pathologies affecting variety of tissues. Thus, such results should be related to complex multi-system reactions, but not the pathologies typically associated with the stomach. Our previous experiments have clearly shown that gastric ulcers strongly affected the enteric nervous system in the stomach wall ^{[15][16][17][18]} and these complex changes differed in several respects from other gastrointestinal pathologies. Importantly, ulcers in the distal part of the stomach (pyloric antrum) affect the gastric emptying ^{[19][20]} leading to maldigestion, malabsorption, and malnutrition. These specific symptoms were even referred to as "pyloric syndrome complex" ^[21].

Since gastric ulcerations affect a huge number of people around the world and, in addition, significantly contribute to the loss of pig livestock production ^{[22][23]}, they represent a serious problem in human and animal medicine. Moreover, the pig—as an omnivorous animal with many embryological, histological, and functional similarities to humans—is considered as the best animal model for biomedical studies on gastrointestinal tract ^{[24][25][26]}. Therefore, the basic science knowledge on substances involved in the regulation of porcine gastric ulcer disease is highly valuable for the future experiments. Thus, in the present experiment we aimed to verify by double immunofluorescence and confocal microscopy whether CART is involved in the stomach enteric nerve's reaction to the gastric antrum ulceration in tissues adjacent to the pathological focus. Importantly, tissue reaction to pathology may be additionally manifested by changes in the expression of genes encoding various substances, and such genetic reaction is of key importance in tissue adaptive changes. The first demonstration of CART mRNA in gastrointestinal tissues was difficult to obtain even in laboratory rodents ^{[27][28]}. To date, no study has described the expression of CART encoding gene in the swine gastrointestinal tract tissues, and neither experiment verified its expression changes under pathological processes occurring in the pig gastrointestinal tube. Therefore, our second scientific aim was to demonstrate the expression of gene encoding CART in the porcine stomach

tissues and verify the changes in its expression under stomach ulcerations using Q-PCR technique (in tissues strictly corresponding with samples tested by immunofluorescence).

2. CART-Immunofluorescence in the Structures of Enteric Nervous System

Microscopic analysis revealed that in all studied animals CART-immunofluorescence was observed mainly in the myenteric perikarya (**Figure 1A–D**) and nerve fibers located within muscular layer (**Figure 1E,G**), while only occasional irregularly arranged submucosal perikarya were noticed in a few individuals of both animal groups (**Figure 2A–D**) and no difference in their occurrence and number was noticed.

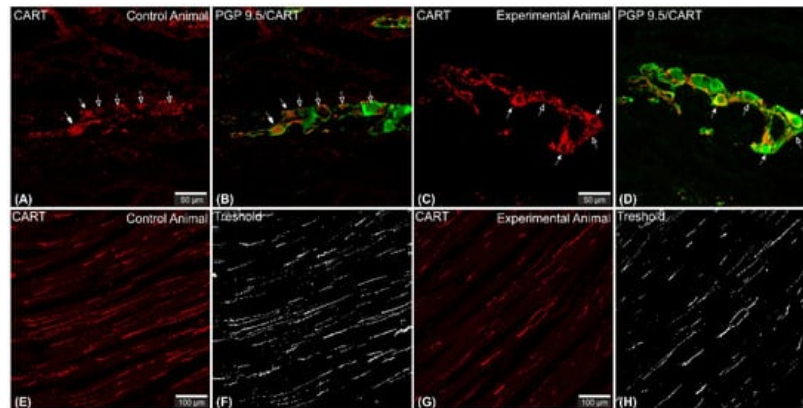


Figure 1. Set of exemplary photomicrographs showing myenteric plexus perikarya (**A–D**; arrows) and nerve fibers (**E,G**) penetrating the circular muscle layer in the control (**A,B,E,F**) and experimental animal (**C,D,G,H**) immunoassayed with antibodies against PGP 9.5 (green channel) and CART (red channel). The number of PGP/CART-IF double immunostained perikarya in experimental animals (**C,D**) was lower than in control pigs (**A,B**). Solid arrows point to highly CART-fluorescent perikarya, empty arrows point to weakly fluorescent cell bodies. In experimental animals perikarya were characterized by stronger immunofluorescence (**C**) than in control ones (**A**). (**E,G**) clearly visible CART-IF varicose nerve fibers penetrating circular muscle layer. (**F,H**) Intermodes threshold method (ImageJ software ver. 1.53c, Rasband, W.S., National Institutes of Health, Bethesda, MD, USA) applied on red channel (CART immunostaining) microphotographs enabled precise quantitative analysis of CART-immunofluorescent nerve fibers in the circular muscle layer indicating their reduction in ulcer animals. Scale bars presented in the pictures.

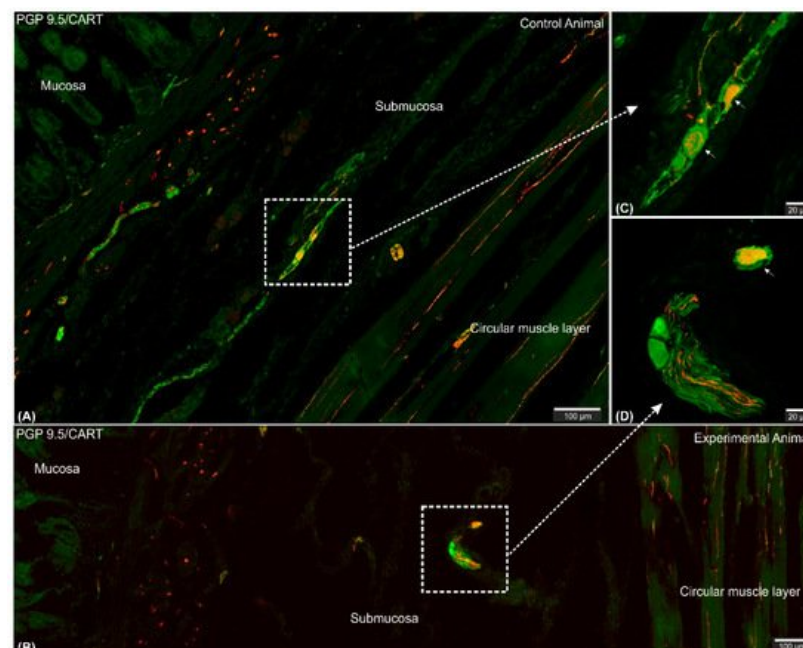


Figure 2. Set of exemplary figures showing submucosal PGP 9.5/CART double immunofluorescent perikarya (arrows) sporadically observed in the control (**A,C**) and experimental (**B,D**) pigs. (**A,B**) Figures showing large area of the stomach wall (mucosa, submucosa, and deeper part of the circular muscle layer) created using the confocal 'tilt' function to visualize the exact location of submucosal perikarya. (**B,D**) Higher magnification of submucosal perikarya. Both channels (red—CART staining, green—PGP 9.5 staining) overlapped in the pictures. Scale bars included in the pictures.

2.1. CART-Immunoreactive Myenteric Plexus Perikarya

CART-immunoreactive perikarya constituted $39.98 \pm 1.24\%$ of myenteric cells in control animals, while in ulcer pigs this number decreased to $34.9 \pm 0.48\%$, and observed difference was statistically significant (**Figure 3**). In both animal groups most of the PGP 9.5/CART-immunofluorescent myenteric perikarya were oval or multipolar in shape, however they differed in dimensions and fluorescence intensity (**Figure 1A–D** and **Figure 4A–D**).

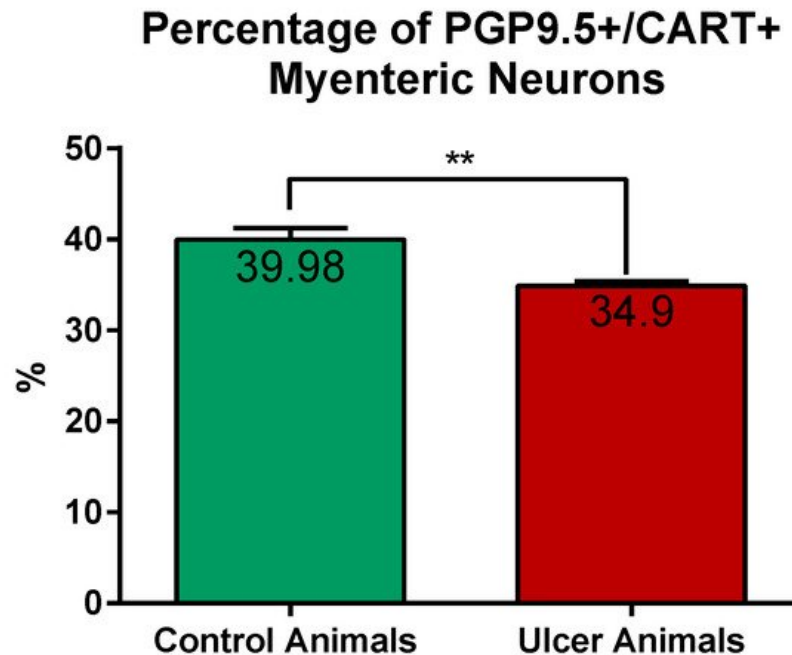


Figure 3. Graph showing the percentage of PGP 9.5/CART double immunofluorescent myenteric perikarya in the control and experimental animals. The number of cells was significantly reduced in ulcer animals. (**) p value = 0.0087.

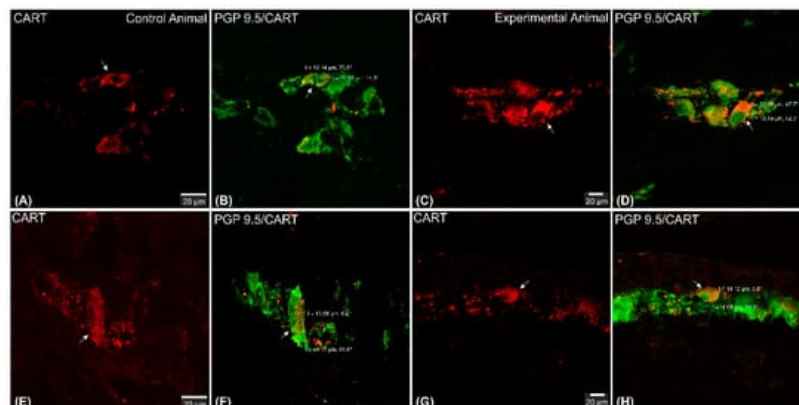


Figure 4. Set of exemplary photomicrographs double immunostained for CART (red channel) and PGP 9.5 (green channel) showing morphology (including dimensions) of double immunofluorescent myenteric perikarya (arrows). (**A–D**)—pictures indicating typical myenteric perikaryon (arrow) observed in the control (**A,B**) and experimental (**C,D**) animals. High intensity of CART-immunofluorescence observed in the experimental animal perikaryon (**C**). (**E,F**) Very large and (**G,H**) small perikarya occasionally observed in both groups of animals. Scale bars included in the pictures. Both channels overlapped in (**B,D,F,H**) pictures. Measurements (long/short axis) made with confocal microscope software and incorporated by graphical software.

Confocal software measurements revealed that in the control animals the average CART-immunofluorescent myenteric perikaryon measured $12.11 \pm 0.28 \times 22.35 \pm 0.44 \mu\text{m}$, while in ulcer pig $13.43 \pm 0.31 \times 24.04 \pm 0.53 \mu\text{m}$, and observed difference was statistically significant (**Figure 5**). However, larger and smaller perikarya were observed in both animal groups (**Figure 4E–H**).

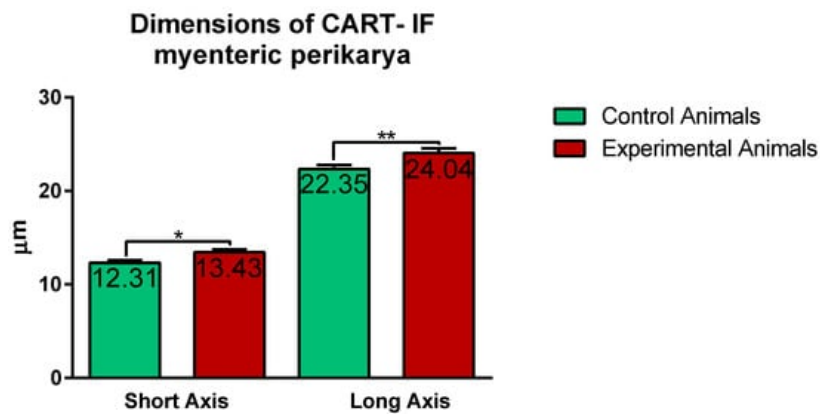


Figure 5. Graph showing the average dimensions (long and short axis) of myenteric perikarya in the control and experimental animals. Both dimensions were increased in ulcer animals. (*) p value = 0.0226; (**) p value = 0.0044.

ImageJ software analysis revealed that in the control pigs average CART-immunofluorescence intensity of myenteric perikarya amounted to 77.25 ± 1.88 units, while in ulcer animals it significantly increased, up to 89.11 ± 3.1 units (**Figure 6**).

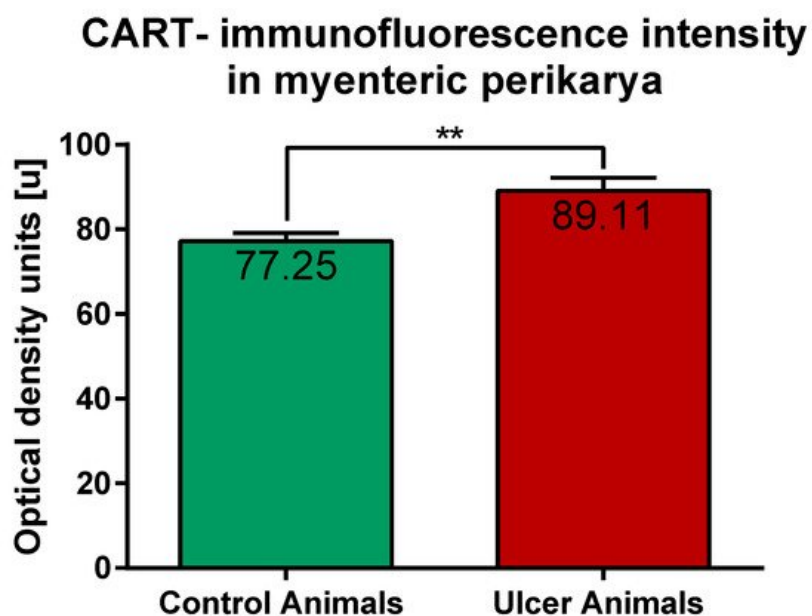


Figure 6. Graph showing the average intensity of CART-immunofluorescence expressed by control and experimental pigs' myenteric perikarya measured with ImageJ software (ver. 1.53c, Rasband, W.S., National Institutes of Health, Bethesda, MD, USA) as a mean grey value inside the cell body area. The values are presented in optical density units. In ulcer animals the average intensity was higher than in control pigs. (**) p value = 0.006.

2.2. CART-Immunoreactive Nerve Fibers

CART-immunoreactive nerve fibers run mostly parallel to muscle fibers. Most numerous CART-immunoreactive nerve fibers were observed within the circular muscle layer. They were characterized by medium to strong immunofluorescence and penetrated the full thickness of the layer (**Figure 1E,G**). ImageJ software analysis of the surface area occupied by CART- fluorescent fibers located in the circular muscular layer (**Figure 1F,H**) revealed its statistically significant decrease from $1.14 \pm 0.08\%$ in control animals to $0.83 \pm 0.06\%$ in experimental pigs (**Figure 7**).

Percentage of surface area occupied by CART-IF fibers in the circular muscle layer

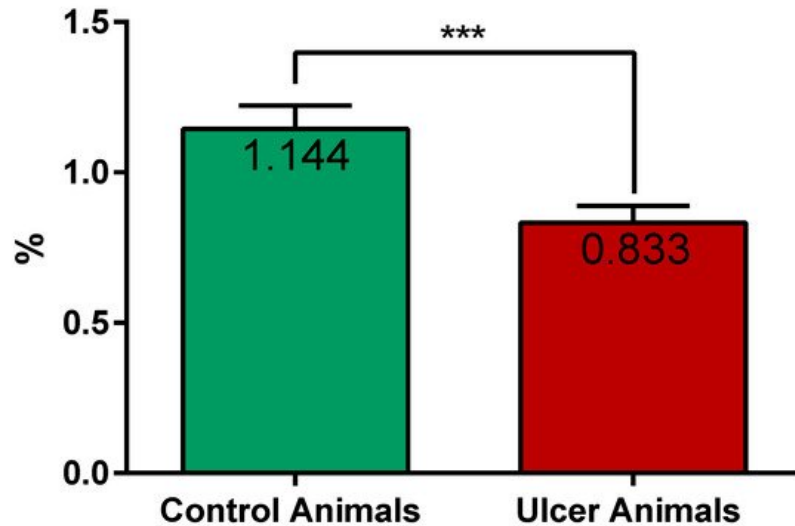


Figure 7. Graph showing the percentage of surface area (in the field of view) occupied by CART-immunofluorescent nerve fibers located in the circular muscle layer in the control and ulcer pigs. The value decreased in animals with ulcers. (***) p value = 0.0006.

In the longitudinal muscle layer, the section thickness of which showed significant differences between different parts of the same specimen, examined nerve fibers were evenly scattered within the layer and no differences in their occurrence were noticed between control and experimental animals (**Figure 8A,B**).

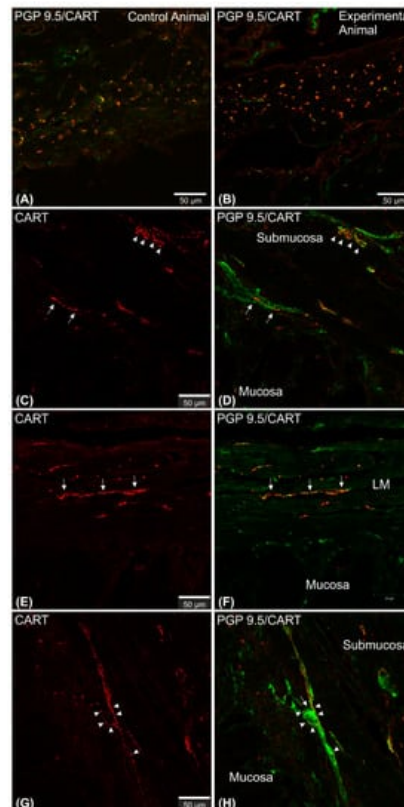


Figure 8. Set of exemplary microphotographs showing CART/PGP 9.5 immunolabelled neuronal fibers in the longitudinal muscle layer (**A,B**) and in the submucosa and lamina muscularis mucosae (**C–H**). (**A,B**) Evenly dispersed, transversally cut neuronal fibers observed in the control (**A**) and experimental (**B**) animals. (**C,D**) Bundles of highly fluorescent varicose nerve fibers located within submucosa (arrowheads) and sparse nerve fibers observed in the lamina muscularis mucosae (arrows) in both studied animal groups. (**E,F**) Thick, highly immunoreactive fibers running parallel to the muscle fibers of muscularis mucosae (arrows) sporadically observed in both groups of animals. (**G,H**) CART-immunofluorescent nerve fibers (arrowheads) attaching and encircling perikaryon located in the lamina muscularis mucosae (arrow) observed in

both studied groups of pigs. Scale bars included in the pictures. CART—red channel, PGP 9.5—green channel. In (A,B,D,F,H) both channels overlapped. LM—lamina muscularis mucosae.

In both animal groups singular, highly CART-immunoreactive neuronal fibers were observed in the submucosa and lamina muscularis mucosae (Figure 8C–F), which run mostly parallel to the muscularis mucosae fibers. Neuronal fibers of these layers frequently bordered or encircled submucosal, CART-negative, perikarya (Figure 8G,H). Occasionally bundles of prominent fibers were additionally noticed (Figure 8E,F) in both animal groups. No CART-immunofluorescent nerve fibers penetrated mucosa in all animals.

2.3. Expression of mRNA Encoding CART in the Stomach Wall

Results of the Q-PCR revealed the expression of gene encoding CART in the stomach tissues of the control and experimental pigs. Statistical analysis of its relative expression (in relation to GAPDH as a housekeeping gene) revealed its significant decrease in stomachs of ulcer animals, in relation to control pigs (Figure 9).

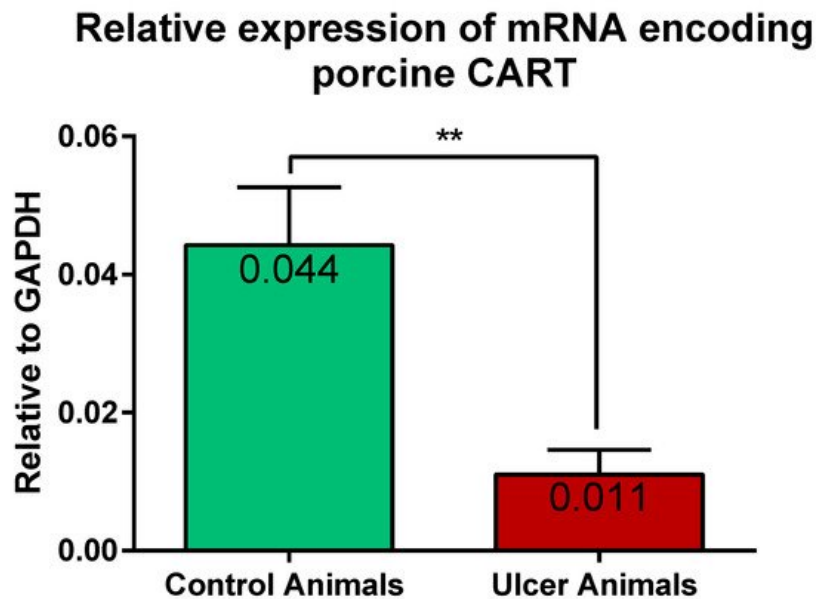


Figure 9. Graph showing the expression level of mRNA encoding CART in the stomach antrum tissues of the control and ulcer pigs. The stomach antrum circular-shaped samples (directly adjacent to the ulcer verge in experimental animals; at the strictly equivalent location in control animals) were cut transversally to the gastric wall and comprised all its layers. The data obtained from each sample were normalized to GAPDH. Relative quantities (RQ) of mRNA were analyzed using the comparative Ct method. (**) p value = 0.0043.

3. Discussion

Our experiment has revealed for the first time that gastric ulceration influenced the CART-dependent intrinsic nerve and tissue reaction. Surprisingly, in the stomach wall adjacent to the ulcer focus the number of CART-immunoreactive myenteric perikarya and the expression of CART-IF in nerve fibers penetrating the muscular circle layer were significantly reduced. Moreover, the dimensions and intensity of CART-fluorescence was changed in myenteric perikarya of ulcer animals. In line, the expression of firstly demonstrated CART encoding mRNA was reduced in studied tissues of ulcer pigs. Perikarya of the submucosal ganglia and neuronal fibers located in the longitudinal muscle layer and submucosa were not engaged in CART reaction to stomach ulcerations.

CART-immunoreactive nerve structures are widely distributed within the enteric nervous system of different species [29]. Interestingly, its expression hugely differs between the part of the digestive tract and species examined [29][30]. Stomach is a specific reservoir of food, in which mechanic mixing coupled with acidic digestion occurs. Moreover, pyloric sphincter in cooperation with pyloric antrum precisely adjusts the flow of chyme to the following parts of the digestive tract (intestines), hugely influencing the proper digestion and absorption of nutrients in the intestines. Therefore, the precise regulation of the stomach motility and gastric juice secretion are of particular importance for proper nutrition and gastrointestinal homeostasis. Until this point, data [11][31][32][33][34][35] as well as obtained neuroanatomical results consistently, suggest that—in healthy individuals CART—is mainly engaged in gastric motility regulation, as depicted by its presence in myenteric perikarya and nerve fibers supplying the muscular layer. Interestingly, the percentage of CART-immunoreactive myenteric perikarya (in relation to all myenteric neurons) varied depending on the stomach compartment studied and the researcher: in the stomach antrum such cells constituted as many as 40% [31]—50% [11]; in the gastric corpus 18% [31][32]—30% [11]

until 46% [42]; and in the pylorus these perikarya accounted for 14% [11] to over 30% [31] of all myenteric neurons. Above described 'site-dependent' discrepancies indicate specific engagement of CART in motor activity regulation in each stomach compartment, while variations regarding the same stomach compartment presented by different authors may result from the precise location of the sample in a given part of the stomach. Porcine stomach is a huge anatomical structure, thus 2–3 cm² specimens sampled for analysis by most of these authors may include unidentical sample localizations, although obtained from the same gastric compartment. In our studies we analyzed the entire transverse cross-section of the pyloric antrum wall (from small to large curvature) in the precisely defined location to obtain the most reliable data. Our results depicted that in the pyloric antrum CART-immunoreactive myenteric perikarya constitute about 40% of all myenteric neurons, strongly suggesting their involvement in the motility regulation in this stomach compartment.

CART-IF neuronal fibers were numerous observed in the muscular layer of the stomach antrum [11][31], corpus [11][12][31][32], pylorus [11][31], and the pyloric antrum, as depicted by our present study, which strongly supports the hypothesis about the influence of CART on the gastric smooth muscle cells functioning under physiological conditions. Since pyloric antrum propulsive activity is engaged in forming an increased pressure of food content necessary for appropriate stomach emptying [36], our neuroanatomical results imply the role of neuronal CART in the regulation of such process. However, immunohistochemical results presented by Zacharko et al. [37], and our earlier tracing study [38] clearly indicate that some of the CART-immunoreactive nerve fibers observed in the porcine gastric wall may originate in dorsal root ganglia and participate in the extrinsic sensory stomach innervation.

In healthy animals, singular, irregularly arranged submucosal CART-immunoreactive gastric perikarya were observed only in sporadic studies (present study; [12][32][39]) or were completely absent [11][31][34][40] suggesting their minor importance for intramural regulation of the stomach mucosa secretory function. The reasonable explanation for the abovementioned minor variations presented by different authors seem to result from tissue sampling differences, as described before.

Interestingly, in the other parts of gastrointestinal tract (in healthy animals), as an esophagus [33] and intestines [40][41], CART-immunoreactive submucosal neurons were encountered, although most of the CART-positive perikarya were also located in the myenteric plexus.

The results of Q-PCR technique obtained in the present experiment demonstrated for the first time the presence of mRNA encoding CART in the stomach of healthy pigs, complementing the existing and only immunocytochemical data on its expression in the gastrointestinal tract of this species [11][12][31][34][40]. Since different mechanisms are engaged in the regulation of mRNA expression and final peptide abundance, the results of Q-PCR technique and immunohistochemistry may vary in the same tissues [42]. Therefore, the presented results are of particular importance, introducing another layer of research on the mechanism of CART expression regulation in the porcine gastrointestinal tract.

References

1. Furness, J.B. *The Enteric Nervous System*; Blackwell: Oxford, UK, 2006.
2. Furness, J.B. The enteric nervous system: Normal functions and enteric neuropathies. *Neurogastroenterol. Motil.* 2008, 20 (Suppl. 1), 32–38.
3. Oponowicz, A.; Kozłowska, A.; Gonkowski, S.; Godlewski, J.; Majewski, M. Changes in the distribution of cocaine- and amphetamine-regulated transcript-containing neural structures in the human colon affected by the neoplastic process. *Int. J. Mol. Sci.* 2018, 19, 414.
4. Rzap, D.; Czajkowska, M.; Całka, J. Neurochemical plasticity of nnos-, vip- and cart-immunoreactive neurons following prolonged acetylsalicylic acid supplementation in the porcine jejunum. *Int. J. Mol. Sci.* 2020, 21, 2157.
5. Burliński, P.J. Inflammation- and axotomy-induced changes in cocaine- and amphetamine-regulated transcript peptide-like immunoreactive (CART-LI) nervous structures in the porcine descending colon. *Pol. J. Vet. Sci.* 2012, 15, 517–524.
6. Bulc, M.; Całka, J.; Zielonka, Ł.; Dabrowski, M.; Palus, K. Effect of chemically-induced diabetes mellitus on phenotypic variability of the enteric neurons in the descending colon in the pig. *Ann. Anim. Sci.* 2020.
7. Rytel, L.; Wojtkiewicz, J.; Snarska, A.; Mikołajczyk, A. Changes in the Neurochemical Characterization of Enteric Neurons in the Porcine Duodenum After Administration of Low-Dose Salmonella Enteritidis Lipopolysaccharides. *J. Mol. Neurosci.* 2020, 1–11.

8. Mikolajczyk, A.; Makowska, K. Cocaine- and amphetamine-regulated transcript (CART) peptide in the nerve fibres of the porcine gallbladder wall under physiological conditions and after Salmonella Enteritidis lipopolysaccharides administration. *Folia Morphol.* 2017, 76, 596–602.
9. Gonkowski, S.; Kamińska, B.; Burliński, P.; Kroll, A.; Calka, J. The influence of drug-resistant ulcerative colitis on the number of cocaine- and amphetamine-regulated transcript peptide-like immunoreactive (CART-LI) mucosal nerve fibres of the descending colon in children. *Prz. Gastroenterol.* 2009, 4, 147–151.
10. Kasacka, I.; Piotrowska, Z. Evaluation of density and distribution of CART-immunoreactive structures in gastrointestinal tract of hypertensive rats. *BioFactors* 2012, 38, 407–415.
11. Bulc, M.; Gonkowski, S.; Calka, J. Expression of Cocaine and Amphetamine Regulated Transcript (CART) in the Porcine Intramural Neurons of Stomach in the Course of Experimentally Induced Diabetes Mellitus. *J. Mol. Neurosci.* 2015, 57, 376–385.
12. Makowska, K.; Gonkowski, S.; Zielonka, L.; Dabrowski, M.; Calka, J. T2 Toxin-Induced Changes in Cocaine- and Amphetamine-Regulated Transcript (CART)-Like Immunoreactivity in the Enteric Nervous System Within Selected Fragments of the Porcine Digestive Tract. *Neurotox. Res.* 2017, 31, 136–147.
13. Palus, K.; Bulc, M.; Calka, J. Effect of acrylamide supplementation on the CART-, VACHT-, and nNOS-immunoreactive nervous structures in the porcine stomach. *Animals* 2020, 10, 555.
14. Makowska, K.; Gonkowski, S. Bisphenol a (Bpa) affects the enteric nervous system in the porcine stomach. *Animals* 2020, 10, 2445.
15. Zalecki, M. The Influence of Antral Ulcers on Intramural Gastric Nerve Projections Supplying the Pyloric Sphincter in the Pig (*Sus scrofa domestica*)—Neuronal Tracing Studies. *PLoS ONE* 2015, 10, e0126958.
16. Zalecki, M. Gastric ulcer induced changes in substance P and Nk1, Nk2, Nk3 receptors expression in different stomach localizations with regard to intrinsic neuronal system. *Histochem. Cell Biol.* 2019, 151, 29–42.
17. Zalecki, M.; Pidsudko, Z.; Franke-Radowiecka, A.; Wojtkiewicz, J.; Kaleczyc, J. Galaninergic intramural nerve and tissue reaction to antral ulcerations. *Neurogastroenterol. Motil.* 2018, 30, e13360.
18. Zalecki, M.; Sienkiewicz, W.; Franke-Radowiecka, A.; Klimczuk, M.; Kaleczyc, J. The influence of gastric antral ulcerations on the expression of Galanin and GalR1, GalR2, GalR3 receptors in the pylorus with regard to gastric intrinsic innervation of the pyloric sphincter. *PLoS ONE* 2016, 11, e0155658.
19. Liebermann-Meffert, D.; Allgower, M. Neuromuscular tissue defects and antropyloric dysfunction in peptic ulcer. *Scand. J. Gastroenterol. Suppl.* 1981, 67, 111–113.
20. Liebermann-Meffert, D.; Muller, C.; Allgower, M. Gastric hypermotility and antropyloric dysfunction in gastric ulcer patients. *Br. J. Surg.* 1982, 69, 11–13.
21. Murray, G.F.; Ballinger, W.F.; Stafford, E.S. Ulcers of the pyloric channel. *Am. J. Surg.* 1967, 113, 199–203.
22. Friendship, R.M. Gastric ulceration in swine. *J. Swine Health Prod.* 2004, 12, 34–35.
23. Melnichouk, S.I. Mortality associated with gastric ulceration in swine. *Can. Vet. J.* 2002, 43, 223.
24. Verma, N.; Rettenmeier, A.W.; Schmitz-Spanke, S. Recent advances in the use of *Sus scrofa* (pig) as a model system for proteomic studies. *Proteomics* 2011, 11, 776–793.
25. Swindle, M.M.; Makin, A.; Herron, A.J.; Clubb, F.J., Jr.; Frazier, K.S. Swine as models in biomedical research and toxicology testing. *Vet. Pathol.* 2012, 49, 344–356.
26. Swindle, M.M. The development of swine models in drug discovery and development. *Future Med. Chem.* 2012, 4, 1771–1772.
27. Douglass, J.; McKinzie, A.A.; Couceyro, P. PCR differential display identifies a rat brain mRNA that is transcriptionally regulated by cocaine and amphetamine. *J. Neurosci.* 1995, 15, 2471–2481.
28. Murphy, K.G.; Abbott, C.R.; Mahmoudi, M.; Hunter, R.; Gardiner, J.V.; Rossi, M.; Stanley, S.A.; Ghatei, M.A.; Kuhar, M.J.; Bloom, S.R. Quantification and synthesis of cocaine- and amphetamine-regulated transcript peptide (79-102)-like immunoreactivity and mRNA in rat tissues. *J. Endocrinol.* 2000, 166, 659–668.
29. Makowska, K.; Gonkowski, S. Cocaine- and Amphetamine-Regulated Transcript (CART) Peptide in Mammals Gastrointestinal System—A Review. *Ann. Anim. Sci.* 2017, 17, 3–21.
30. Ekblad, E. CART in the enteric nervous system. *Peptides* 2006, 27, 2024–2030.
31. Zacharko-Siembida, A.; Arciszewski, M.B. Immunoreactivity to cocaine- and amphetamine-regulated transcript in the enteric nervous system of the pig and wild boar stomach. *Anat. Histol. Embryol.* 2014, 43, 48–55.

32. Rekawek, W.; Sobiech, P.; Gonkowski, S.; Zarczynska, K.; Snarska, A.; Wasniewski, T.; Wojtkiewicz, J. Distribution and chemical coding patterns of cocaine- and amphetamine-regulated transcript-like immunoreactive (CART-LI) neurons in the enteric nervous system of the porcine stomach cardia. *Pol. J. Vet. Sci.* 2015, 18, 515–522.
33. Kasacka, I.; Piotrowska, Z.; Car, H.; Janiuk, I.; Lebkowski, W. Cocaine- and amphetamine-regulated transcript: Identification and distribution in human gastrointestinal tract. *J. Biol. Regul. Homeost. Agents* 2012, 26, 419–428.
34. Wierup, N.; Gunnarsdóttir, A.; Ekblad, E.; Sundler, F. Characterisation of CART-containing neurons and cells in the porcine pancreas, gastro-intestinal tract, adrenal and thyroid glands. *BMC Neurosci.* 2007, 8, 51.
35. Ekblad, E.; Kuhar, M.; Wierup, N.; Sundler, F. Cocaine- and amphetamine-regulated transcript: Distribution and function in rat gastrointestinal tract. *Neurogastroenterol. Motil.* 2003, 15, 545–557.
36. Armitage, A.K.; Dean, A.C.B. Function of the pylorus and pyloric antrum in gastric emptying. *Gut* 1963, 4, 174–178.
37. Zacharko-Siembida, A.; Kulik, P.; Szaluk, R.; Lalak, R.; Arciszewski, M.B. Co-expression patterns of cocaine- and amphetamine-regulated transcript (CART) with neuropeptides in dorsal root ganglia of the pig. *Acta Histochem.* 2014, 116, 390–398.
38. Zalecki, M. Extrinsic primary afferent neurons projecting to the pylorus in the domestic pig—Localization and neurochemical characteristics. *J. Mol. Neurosci.* 2014, 52, 82–89.
39. Kozłowska, A.; Godlewski, J.; Majewski, M. Distribution patterns of cocaine-and amphetamine-regulated transcript-and/or galanin-containing neurons and nerve fibers located in the human stomach wall affected by tumor. *Int. J. Mol. Sci.* 2018, 19, 3357.
40. Rychlik, A.; Gonkowski, S.; Nowicki, M.; Calka, J. Cocaine- and amphetamine-regulated transcript immunoreactive nerve fibres in the mucosal layer of the canine gastrointestinal tract under physiological conditions and in inflammatory bowel disease. *Vet. Med.* 2015, 60, 361–367.
41. Wojtkiewicz, J.; Gonkowski, S.; Bladowski, M.; Majewski, M. Characterisation of cocaine-and amphetamine-regulated transcript-like immunoreactive (CART-LI) enteric neurons in the porcine small intestine. *Acta Vet. Hung.* 2012, 60, 371–381.
42. Vogel, C.; Marcotte, E.M. Insights into the regulation of protein abundance from proteomic and transcriptomic analyses. *Nat. Rev. Genet.* 2012, 13, 227–232.

Retrieved from <https://encyclopedia.pub/entry/history/show/29533>